Zeitschrift: Helvetica Physica Acta
Band: 58 (1985)
Heft: 1

Artikel: Dislocations in solids investigated by means of nuclear magnetic resonance

Autor: Hosson, J.Th.M. de

DOI: https://doi.org/10.5169/seals-115579

Helvetia Physica Acta
Vol. 58, 1985 42-59

0018-0238/85/010042-18$1.50+0.20/0

DISLOCATIONS IN SOLIDS INVESTIGATED BY MEANS OF NUCLEAR MAGNETIC RESONANCE

J. Th. M. De Hosson

Dept. of Applied Physics, Materials Science Centre, University of Groningen, Nijenborgh 18, 9747 AG Groningen, The Netherlands.

The intricate details of the mode of dislocation movement in a stress field and the mobile fraction of the total number of dislocations in a material are measured by means of combined plastic deformation and NMR experiments. It turned out that pulsed nuclear magnetic resonance is a complementary new technique for the study of moving dislocations in metallic and ionic crystals.

1. Introduction

The development of magnetic resonance spectroscopy ranks among one of the most important advances in chemical and solid state physics during the past three decades. The great strength of nuclear magnetic resonance is that the resonance signal is characteristic of the particular nucleus being studied. Because the nuclei of many elements are characterized by intrinsic magnetic moments, the resonance frequency ω_o, in a magnetic field $\vec{H}_o$, equals γH_o, where the gyromagnetic ratio γ is a constant which is different for different nuclei. For this reason, NMR can be used to measure properties which belong exclusively to the nuclei whose motions are of interest. Moreover, the surrounding of a nucleus may affect NMR properties like, linewidth, relaxation time etc. Accordingly, NMR can be used to study the environment of the nuclei providing microscopic information of atomic motions.

The principal aim of our research is to gain some insight in atomic motions which play a keyrole in phenomenon of slip in crystals and in the mechanism of the process of plastic deformation. It has been well established

that the plastic deformation of solid materials is brought about by the movement of dislocations. Because the process of dislocation motion is made up of atomic movement nuclear magnetic resonance techniques should offer a possibility to determine the way in which dislocations progress through the crystal as a function of time utilizing spin-lattice relaxation as a tool. For a comprehensive theoretical survey of the dislocation induced relaxation, reference should be made to our review [1]. We have shown that nuclear magnetic resonance (NMR) is a useful tool for 'in situ' investigations of dislocation motion in non-metallic materials as well as in (pure) polycrystalline metals. In the work, the nuclear spin relaxation rate in the rotating frame, $T_{1\rho}^{-1}$, has been instantaneously measured while a sample is being plastically deformed with a constant deformation rate $\dot{\varepsilon}$. It turned out that from these pulsed nuclear magnetic resonance experiments three microscopic informations of the dislocation motion can be deduced in principle: (i) the mean free path of moving dislocations; (ii) the mean time of stay between two consecutive jumps of a mobile dislocation, and (iii) the mobile dislocation density as a fraction of the total dislocation density. Moreover, quadrupolar broadening of the nuclear magnetic resonance lines provided information of: (iv) the total dislocation density.

While static quadrupolar effects associated with static lattice defects such as dislocations are analyzed in terms of width, line shape and intensity of the NMR signal, dynamical effects, such as dislocation motion during plastic deformation, are studied through the related nuclear spin-lattice relaxation process. Nevertheless, both experimental methods are essentially based on the interaction between nuclear electric quadrupole moments and electric quadrupole moments and electric field gradients at the nucleus. Around a dislocation in a cubic crystal the symmetry is destroyed and interactions between nuclear electric quadrupole moments and electric field gradients arise. Whenever a dislocation changes its position in the crystal, the surrounding atoms have also to move, thus causing time fluctuations both of the quadrupolar and dipolar spin Hamiltonian for spins with $I > \frac{1}{2}$. However, dipolar effects on the nuclear spin relaxation due to dislocation motion are negligible and quadrupolar interactions dominate the observed relaxation behaviour. Furthermore, for the investigation of rather infrequent defect motions as in the case of moving dislocations, the spin-lattice relaxation time in the rotating frame,

$T_{1\rho}$, has proved to be the most appropriate NMR parameter affected by such motions.

2. Theoretical Background

In the following we will focus mainly on plastic deformation experiments with a constant strain rate $\dot{\varepsilon}$. This type of experiment is governed by Orowan's equation [2]:

$$\dot{\varepsilon} = \phi \, b \, \rho_m \frac{L}{\tau_w} , \tag{1}$$

assuming a thermally activated, jerky motion of mobile dislocations of density ρ_m. The motion may be considered to be jerky-like, if the actual jump time τ_j is small compared to the meantime of stay τ_w at an obstacle. In Eq. (1), ϕ denotes a geometrical factor, b symbolizes the magnitude of the Burgers vector and L is the mean jump distance between obstacles which are considered to be uniform.

While deforming a sample with a constant strain rate $\dot{\varepsilon}$ the spin-lattice relaxation rate in a weak rotating field H_1 ('locking field'), $1/T_{1\rho}$, of the resonant nuclei in the sample is enhanced due to the motion of dislocations. The resulting total relaxation rate may be decomposed into a background relaxation rate, $(1/T_{1\rho})_o$ and the contribution $(1/T_{1\rho})_D$ which is governed by the mechanism of dislocation motion, i.e. by equation (1)

$$\frac{1}{T_{1\rho}} = \left(\frac{1}{T_{1\rho}}\right)_o + \left(\frac{1}{T_{1\rho}}\right)_D . \tag{2}$$

In metals and alloys, $(1/T_{1\rho})_o$ is due to fluctations in the conduction electron-nucleus interaction leading to the Korringa relation $(T_{1\rho})_o.T = c$, where the magnitude of the constant c depends slightly on the strength of the locking field H_1. In table I the actual values of c are given for samples under investigation, measured at T = 77 K (see section 3).

At a finite plastic strain rate, dislocations move in the crystal, i.e. causing time fluctuations both of the quadrupolar and dipolar spin Hamiltonian for spins with $I > \frac{1}{2}$. However, the dipolar effects on the resulting nuclear spin relaxation due to dislocation motion are negligible and quadrupolar interactions dominate the relaxation behaviour. Furthermore, in the range of deformation rates applied here the atomic movements involved in

dislocation motion are in the so-called ultra-slow motion region, where the Zeeman spin-lattice relaxation rate T_1^{-1} and the spin-spin relaxation rate T_2^{-1} are not remarkably influenced by dislocation motion and where the rotating-frame relaxation rate $T_{1\rho}^{-1}$ is the most appropriate NMR parameter affected by such motions.

Table I. Values of Korringa constants c and of local fields in the rotating frame, $H_{L\rho}$, of ^{27}Al in aluminium samples under investigation, measured at 77K

System	c.$^{\cdot}$ [Ks]	$H_{L\rho}$(G)
5N aluminium	1.85±0.1	3.16±0.6
Al:0.1 at.%Cu	1.85±0.1	3.3 ±0.6
Al:0.5 at.%Cu	1.95±0.1	3.9 ±0.8
Al:1 at.%Cu	2.05±0.1	4.4 ±0.9

The resulting expression for the relaxation rate $(1/T_{1\rho})_D$ induced by dislocation motion is given by [1]

$$\left(\frac{1}{T_{1\rho}}\right)_D = \frac{\delta_Q}{H_1^2 + H_{L\rho}^2} \cdot \langle V^2 \rangle \cdot g_Q(L) \cdot \frac{\rho_m}{\tau_w} \tag{3}$$

Here

$$\delta_Q = \frac{3}{320} \cdot \left(\frac{eQ}{\gamma\hbar}\right)^2 \cdot \frac{2I + 3}{I^2(2I - 1)} \tag{4a}$$

is a quadrupole coupling constant (Q:nuclear quadrupole moment, I:nuclear spin, γ: gyromagnetic ratio) and $\langle V^2 \rangle$ denotes the second moment of the electric field gradient due to the stress field of a dislocation of unit length.

In continuum approximation, $\langle V^2 \rangle$ may be expressed as

$$\langle V^2 \rangle = \int_{r_c}^{R_o} \int_{o}^{2\pi} r \, dr \, d\theta V^2(r,\theta), \tag{4b}$$

where $V(r,\theta)$ is the electric field gradient at a nuclear site with coordinates (r,θ) with respect to a given dislocation, the inner cut-off radius r_c is given by $r_c \simeq 3b$, and the outer cut-off radius R_o is determined by the total density of the dislocations, ρ_T: $R_o = (\pi.\rho_T)^{-\frac{1}{2}}$. $H_{L\rho}$ is the mean local field in

the rotating frame determined by the local dipolar field $H_{D\rho}$ and the local quadrupolar field $H_{Q\rho}$

$$H_{L\rho}^2 = H_{D\rho}^2 + H_{Q\rho}^2 . \qquad (4c)$$

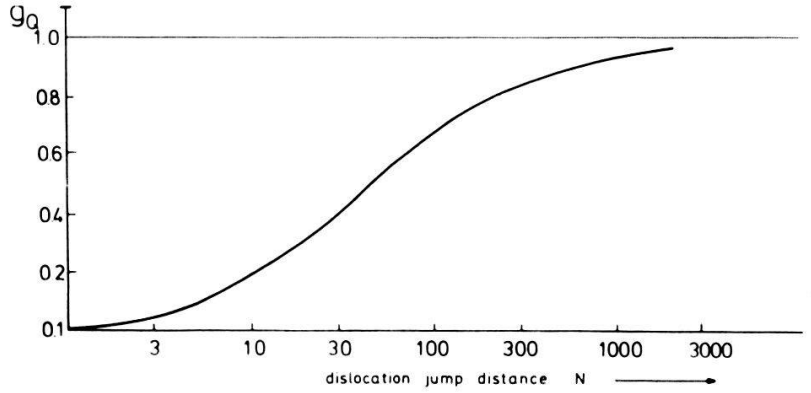

Fig. 1. Quadrupolar geometry factor g_Q for a mobile dislocation as a function of the normalized jump distance N (in units of the Burgers vector).

The quadrupolar geometry factor $g_Q(L)$ in equation (3) which depends on the mean step width L is presented in Fig. 1 where the jump distance L is expressed in units of the Burgers vector b: N = L/b. Typically, in plastic deformation experiments the jump distance L is of the order of $10^{-5} \div 10^{-4}$cm, i.e. N is of the order of 10^3. For such large jump distances $g_Q(L)$ approaches to one being not very sensitive to a change in L. Furthermore, in the following we will assume that $g_Q(L)$ is not a sensitive material-dependent quantity.

It has to be noted, that equation (3) is valid only in the 'strong-collision region' where the dislocation motion is slow enough to allow the spins to establish a common spin temperature between successive dislocation jumps. In practice, the condition is fulfilled for strain rates $\dot{\varepsilon}$ up to about $10s^{-1}$ depending slightly on $H_1^2 + H_{L\rho}^2$.

For ^{27}Al in aluminium, the quadrupole coupling constant δ_Q (equation (4a)) has the value (Q = 0.15 barn; $\gamma = 7.035.10^3\ G^{-1}\ s^{-1}$) 2.85 . $10^{-25} G^2\ dyne^{-1}\ cm^4$. The value of $\langle V^2 \rangle$ may either be determined theoretically by means of the corresponding theoretical expression of $V(r,\theta)$ for dislocations as given by Kanert and Mehring [3] or derived experimentally from analysis of the

line shape of the NMR signal of the sample which is quadrupole distorted by a known number of dislocations. In the first case, starting from $V(r,\theta) = \mu b/2\pi \cdot C_{11}\langle f^2(\theta)\rangle^{\frac{1}{2}} \cdot r^{-1}$ (μ: shear modulus, C_{11}: gradient-elastic constant, $f(\theta)$: orientation function) equation (4b) may be rewritten as

$$\langle V^2\rangle = \frac{1}{2\pi}(\mu . b . C_{11})^2 . \langle f^2\rangle . \ln\frac{R_o}{r_c} . \qquad (5)$$

Then, for ^{27}Al in aluminium the mean-squared EFG $\langle V^2\rangle$ of a dislocation of unit length is given by ($b = 2.86 \cdot 10^{-8}$ cm, $\rho_T = 10^{10}$ cm^{-2}, $C_{11} = 7.10^3$ dyne$^{-\frac{1}{2}}$, $\mu = 2.8 \cdot 10^{11}$ dyne cm^{-2} $\langle V^2\rangle = 1.05 \cdot 10^{15}$ dyne cm^{-2} or, introducing the quadrupole factor $A_Q = \delta_Q . \langle V^2\rangle$: $A_Q|\text{Theory} = 3.0 \cdot 10^{-10}$ G^2 cm^2. On the other hand, A_Q is shown to be given by the relation:

$$A_Q = \frac{\langle H_Q^2\rangle}{\rho_T} , \qquad (6)$$

where $\langle H_Q^2\rangle$ denotes the mean-squared local quadrupole field due to dislocations of total density ρ_T. From experimental NMR and X-ray data in plastically deformed aluminium, as published by Kanert and Preusser [4] both $\langle H_Q^2\rangle$ and ρ_T can be estimated roughly: $\langle H_Q^2\rangle = 8.25$ G^2; $\rho_T \simeq 2.8 \cdot 10^{10}$ cm^{-2}. Therefore, $A_Q|\text{Exp.} = 2.95 \cdot 10^{-10}$ G^2 cm^2. Comparison of the two values for A_Q determined independently shows a fair agreement. Finally, combining Orowan's relation (1) with equation (3) one obtains

$$\left(\frac{1}{T_{1\rho}}\right)_D = \frac{A_Q}{H_1^2 + H_{L\rho}^2} \cdot \frac{1}{\phi . b} \cdot \frac{g_Q(L)}{L} \dot{\varepsilon} . \qquad (7)$$

Hence, for a given plastic-strain rate $\dot{\varepsilon}$ the dislocation induced spin relaxation rate is proportional to the inverse of the mean jump distance L. This relationship is used in the experiments discussed below to determine L.

3. Experimental details

In the NMR experiment, the sample under investigation is plastically deformed by a servo-hydraulic tensile machine (ZONIC Technical Lab. Inc. Cincinnati) of which the exciter head XCI 1105 moves a driving rod with a constant velocity. While the specimen was deforming, ^{27}Al nuclear spin measurements were carried out by means of a BRUKER pulse spectrometer SXP 4-100

operating at 15.7 MHz corresponding to a magnetic field of 1.4 T controlled by an NMR stabilizer (BRUCKER B-SN 15). The NMR head of the spectrometer and the frame in which the rod moves formed a unit which was inserted between the pole pieces of the electromagnet of the spectrometer. A scheme of the experimental set-up is displayed in Fig. 2. As shown in this block diagram, the spectrometer was triggered by the electronic control of the tensile machine. The trigger starts the nuclear spin relaxation experiment at a definite time during the deformation determined by the delay time of the trigger pulse. Immediately before and after the plastic deformation the magnitude of the background(conduction-electron) relaxation time $(T_{1\rho})_o$ was measured. From the experimental $T_{1\rho}$-data, the dislocation induced contribution of the relaxation time, $(T_{1\rho})_D$, could be determined (eq. 2).

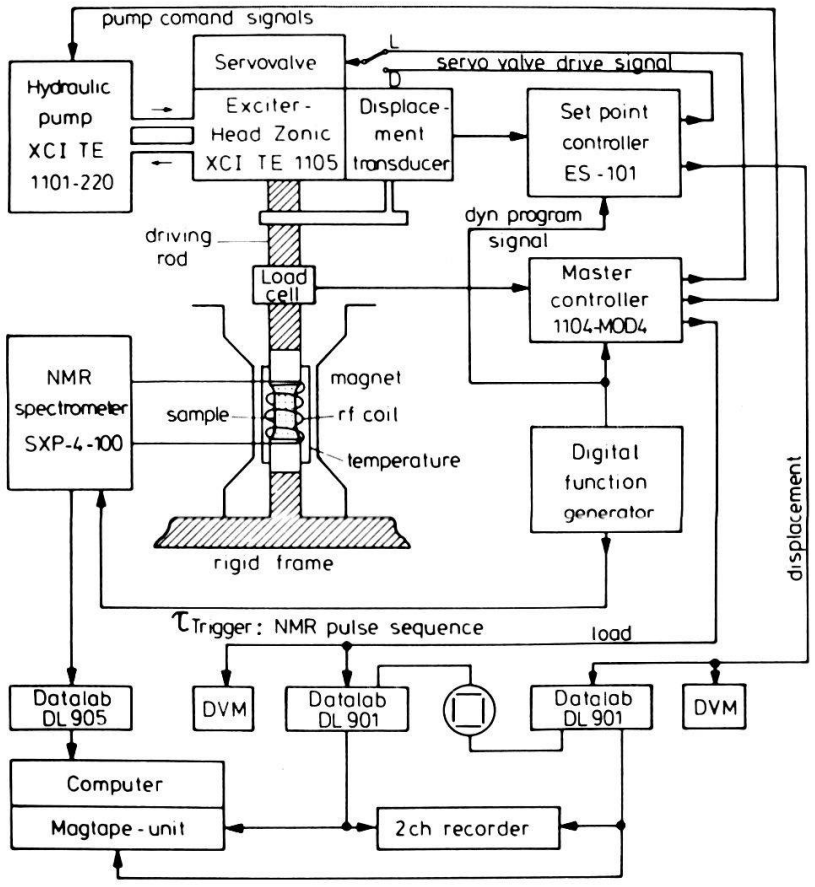

Fig. 2. Block diagram of the experimental set-up.

In the following the efficiency of the total system is demonstrated by an in situ experiment carried out under extreme conditions. The experiment was performed on a single rectangular ultrapure (5N) aluminium foil of size 27 mm x 12 mm x 50 μm in order to study the microscopic details of dislocations in the specimen. The deformation rate of the sample during the actual experiment was very large, namely 1.6 s^{-1}. Figure 3 shows the acting load P, the resulting displacement Δx, the rf pulse sequence consisting of a π/2 pulse followed by a locking field H_1, and the ^{27}Al free induction signal F(t) in the experiment as a function of time.

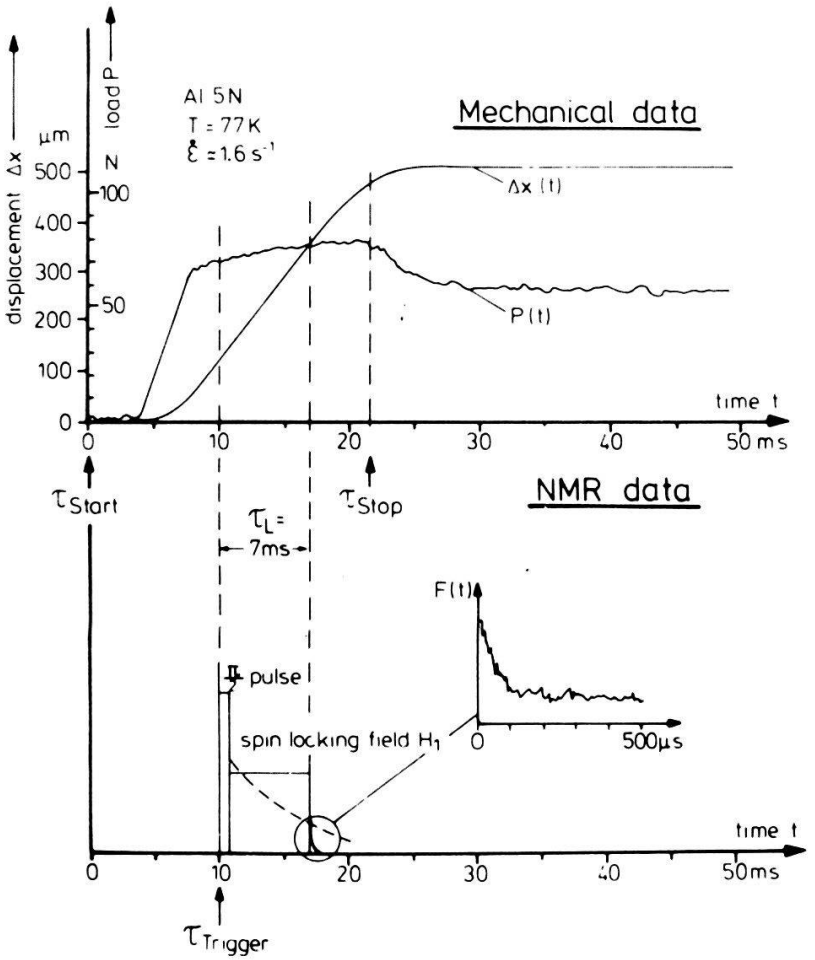

Fig. 3. Displacement Δx, load P, rf-pulse sequence (π/2 pulse followed by a locking field of strength H_1), and ^{27}Al free inducting decay signal F(t) as a function of time during an in situ NMR tensile experiment on an aluminium foil (see text).

The rf sequence which measures the spin-lattice relaxation time in the rotating frame, $T_{1\rho}$, of the ^{27}Al nuclei (see also Fig. 4) is applied after the delay time $\tau_{Trigger}$.

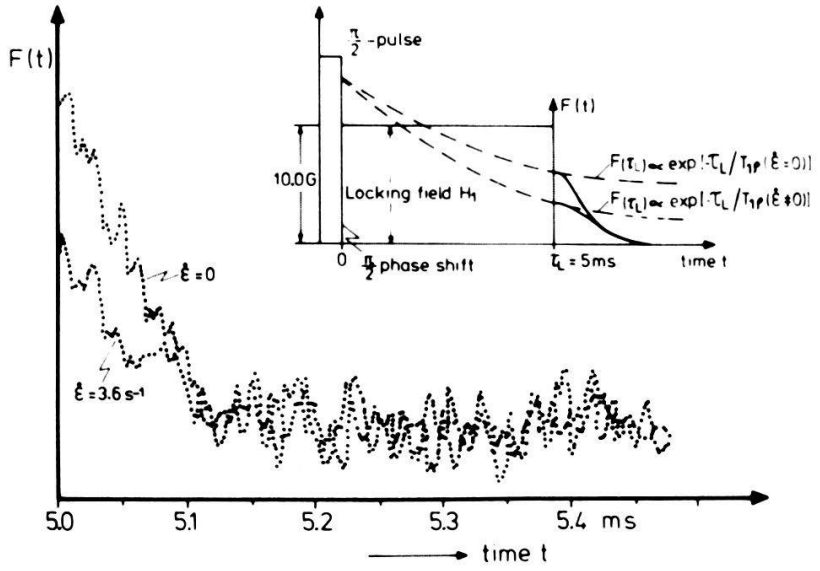

Fig. 4. Result of an in situ NMR tensile experiment showing the ^{27}Al free induction decays F(t) in aluminum after a spin-locking sequence with zero and finite plastic strain rate $\dot{\varepsilon}$. From the measurement $T_{1\rho}(\dot{\varepsilon}=0)$ = 25.0 ms and $T_{1\rho}(\dot{\varepsilon}=3.6\ s^{-1})$ = 7.2 ms is obtained.

The delay is determined by the duration of the pure elastic deformation which can be obtained by the P(t) curve. The trigger signal is generated by the digital function generator (see Fig. 2). As depicted in Fig. 3, the $T_{1\rho}$ measurement is carried out in a short time interval of 7 ms, where the displacement Δx is proportional to time t, resulting in a constant deformation rate of the sample of 1.6 s^{-1}. Furthermore, the acting load P is nearly constant at that time interval, particularly for stage II of the stress-strain curve of aluminium.Figure 4 shows further details of the single shot $T_{1\rho}$ measurement during the actual deformation carried out by means of the spin-locking technique. A $\pi/2$ pulse with an rf field large compared to the local fields in the sample along the x direction rotates the nuclear magnetization from the direction of the static magnetic field to the y direction. Immediately after the pulse, the rf field is phase shifted by $\pi/2$ and reduced to a value of H_1.

Now H_1 lies parallel to the direction of the nuclear magnetization; the magnetization is called "locked" in a frame rotating with the Larmor frequency ω_o. With respect to the rotating frame, H_1 plays the role of a time-independent field. Consequently, the rotating magnetization relaxes parallel to the locking field H_1 with a time constant $T_{1\rho}$, the relaxation time in the rotating frame. To measure $T_{1\rho}$, the nuclear magnetization is allowed to decrease in the presence of the locking field H_1 for some time t, then H_1 is turned off and the initial height (or the total area) of the nuclear free induction decaz signal F(t) is measured. According to Fig. 4 one has for $t = \tau_L$

$$F(\tau_L) = F(0) \exp(-\tau_L/T_{1\rho}). \qquad (8)$$

The figure shows the free induction decays F(t) after the spin-locking sequence with $\dot{\varepsilon} = 0$ and with $\dot{\varepsilon} = 3.6\ s^{-1}$, a finite plastic strain rate. Obviously an applied strain rate $\dot{\varepsilon}$ causes a significant reduction in the relaxation time $T_{1\rho}$ due to the motion of dislocations. An evaluation of the experiment leads to $T_{1\rho}(\dot{\varepsilon} = 0) = 25.0$ ms and $T_{1\rho}(\dot{\varepsilon} = 3.6\ s^{-1}) = 7.2$ ms, respectively. According to Eq. (2), from both the data, a dislocation induced contribution to the relaxation of $100\ s^{-1}$ is obtained.

It should be noted that a larger number of different investigations on dislocation dynamics has been carried out in the past by means of the NMR tensile testing apparatus described here. Detailed information of certain NMR experiments along these lines on metallic (Al-base alloys) and ionic crystals can be obtained from ref [5-12]. In the following we will present only some results of pure Al as a typical example. For a quantitative evaluation of the spin-lattice relaxation rate $(T_{1\rho}^{-1})D$ as a function of $\dot{\varepsilon}$, numerical values of the local fields $H_{L\rho}$, $H_{D\rho}$ and $H_{Q\rho}$ are needed (see Eq. 7).

In order to obtain the static local field $H_{D\rho}$ and $H_{Q\rho}$, respectively, of the samples [see equations (3) and (4c)] the ^{27}Al spin echo signal of each sample was measured. For I = 5/2 (the nuclear spin quantum number of ^{27}Al) a $\pi/2$-τ-40^o pulse sequence induces a spin echo signal at $t = 2\tau$ which may be expressed in a normalized representation as

$$E(t) = 0.247 \cdot D(t) + (0.469 \cdot Q(2t) + 0.284 \cdot Q(4t)) \cdot D(t) \qquad (9a)$$

with E(0) = 1. Here D(t) denotes the Fourier cosine transformation of the dipolar broadening function $g_D(\omega)$ and Q(t) is the corresponding transform of the

quadrupole broadening function $g_Q(a)$.

$$D(t) = \int_{-\infty}^{+\infty} g_D(\omega) \cos(\omega t)\, d\omega;\ D(0) = 1 \tag{9b}$$

$$Q(nt) = \int_{-\infty}^{+\infty} g_Q(a)\cos(n\cdot at)\, da;\ Q(0) = 1;\ n = 2,4 \tag{9c}$$

[see equation 9a)]

where the quadrupole distortion frequency a is given by

$$a = \frac{3eQ}{4I(2I - 1)\hbar} \cdot V_{zz} \tag{10}$$

(V_{zz}: component of the electric field gradient tensor due to lattice distortions in the direction of the external magnetic field). The dipolar function D(t) as well as the quadrupolar function Q(t) can be expressed to a fair approximation by Gaussian functions

$$D(t) = \exp\left(-\frac{\Delta_D^2}{2} t^2\right) \tag{11a}$$

$$Q(t) = \exp\left(-\frac{\Delta_Q^2}{2} \cdot t^2\right) \tag{11b}$$

where Δ_D^2 and Δ_Q^2 are the second moments of the dipolar broadening function $g_D(\omega)$ and of the quadrupolar broadening function $g_Q(a)$, respectively. From the second moments, the local fields in the rotating frame can be obtained by using the general relation [13]

$$H_{L\rho}^2 = \frac{1}{3} \Delta^2 \ . \tag{12}$$

An example of a spin echo signal is given in Fig. 5. The figure shows the spin echo signal of ^{27}Al in an Al:1 at.% Cu alloy. The second moments Δ_D^2 and Δ_Q^2 were determined by fitting the measured echoes of the different samples by means of equation (9a). The analysis leads to a value for the dipolar second moment Δ_D of about 3.3 G. Contrary to the dipolar second moment Δ_D^2, the quadrupolar second moment Δ_Q^2 depends on the lattice distortion in the sample due to dislocations and impurity atoms like copper. Therefore, the total local field in the rotating frame, $H_{L\rho}$, increases slightly with increasing concentration of copper in the samples. This is shown in Table I where $H_{L\rho}$ was determined from the experimental data Δ_D, and Δ_Q by means of $H_{L\rho} = 1/\sqrt{3}.\ (\Delta_D^2 + \Delta_Q^2)$ (see Eq. 12). According to eq. (7), in the strong collission region, a plot of the dislocation-induced contribution to $T_{1\rho}$ vs square of the locking field will yield a

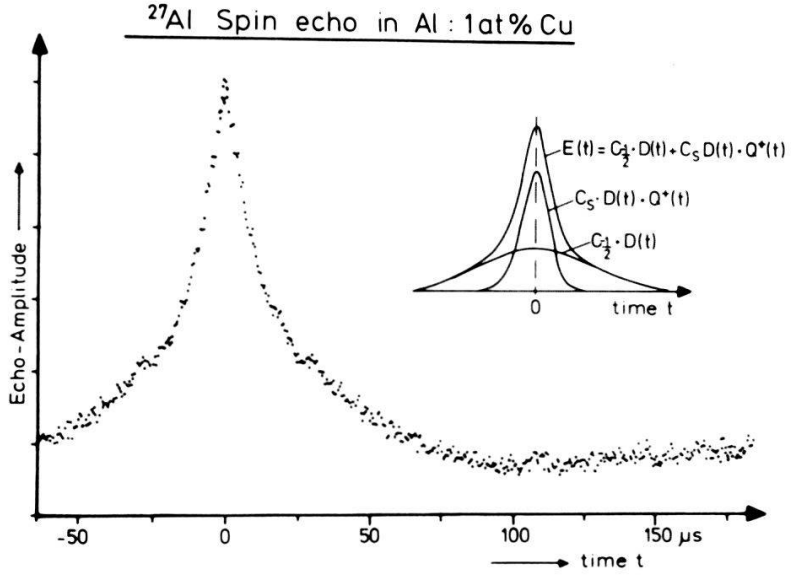

Fig. 5. ^{27}Al spin echo in Al:1 at.% Cu at 77K. For I=5/2 $C_{-\frac{1}{2}}$=0.247 and $C_s Q^+(t)$=0.469 Q(2t)+0.284 Q(4t), see equation 9a.

straight line which can be extrapolated to find the abscissa-intercept at $H_1^2 = -H_{L\rho}^2$. Figure 6 shows such a plot of $(T_{1\rho})_D$ of ultrapure ^{27}Al at a constant $\dot{\varepsilon}$. The local field $H_{L\rho}$ thus obtained is $H_{L\rho}$=3.16G in line with the data obtained from the line shape analysis of the spin echo signals (see Table I) in the Al-Cu alloys.

In Fig. 7 the dislocation-induced contribution to the relaxation rate, $(1/T_{1\rho})_D$, measured with a constant locking field H_1 of 10G is plotted as a function of plastic strain rate $\dot{\varepsilon}$ for two different temperatures (77 K and 298 K). The slope of the curve up to $\dot{\varepsilon} = 10s^{-1}$ is found to be proportional to the strain rate $\dot{\varepsilon}$ as predicted by equation (7). As discussed in section 2, from the magnitude of the ratio $(1/T_{1\rho})_D/\dot{\varepsilon}$ the mean jump distance L can be determined if the other parameters in equation (7) are known. Based on such experiments systematic measurements of the jump distance L in the different aluminium samples were investigated in relation to transmission electron microscopic investigations.

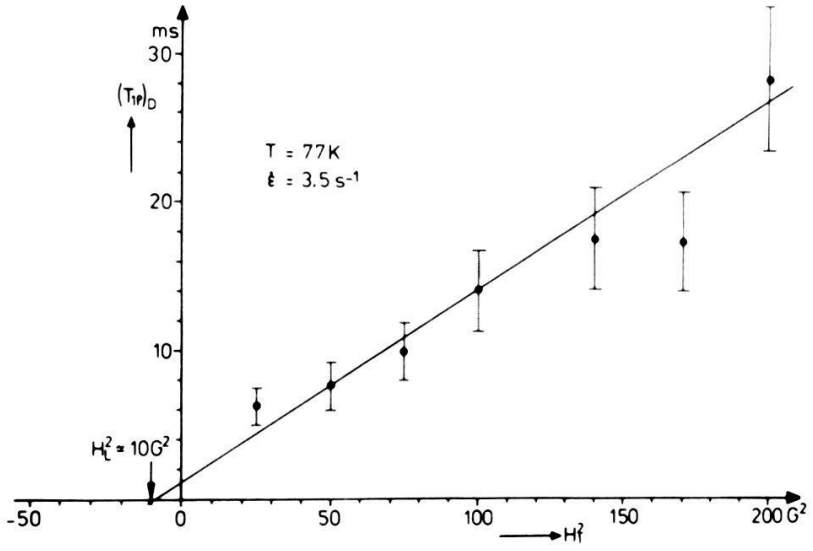

Fig. 6. Plot of the dislocation-induced contribution to the relaxation time $T_{1\rho}$ vs the locking field H_1^2 of ^{27}Al at a constant strain rate $\dot{\epsilon}$ at 77 K.

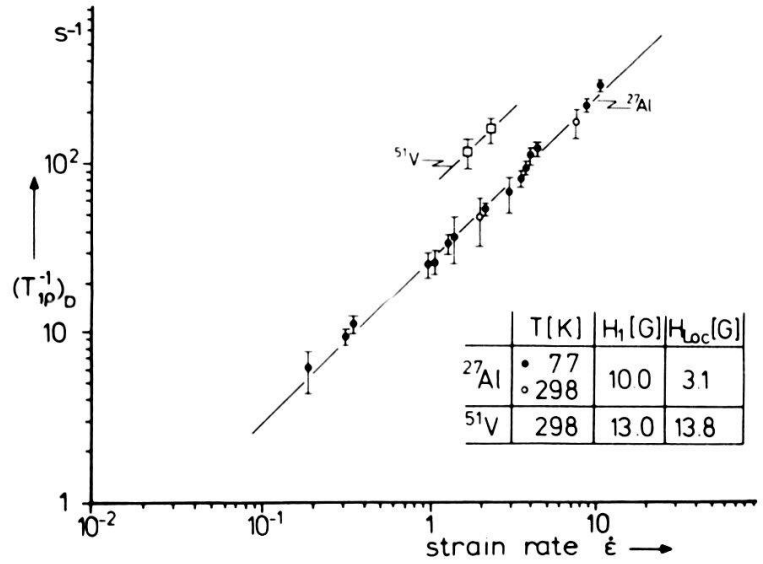

Fig. 7. Dislocation-induced part of the ^{27}Al and ^{51}V relaxation rates $(T_{1\rho}^{-1})_D$ in aluminium and vanadium as a function of $\dot{\epsilon}$ for different temperatures $(\epsilon \gtrsim 7\%)$.

4. Results and Discussion

As discussed above, from the magnitude of the slope of the curve $(T_{1\rho}^{-1})_D$ vs $\dot{\varepsilon}$ the mean jump distance L can be obtained provided the other parameters in equation (7) are known. Taking the Schmid factor ϕ for polycrystalline f.c.c. material equal to 0.33 and the data as given in section 3, the mean jump distance calculated from Fig. 7 is about 0.1 μm for $\varepsilon \gtrsim 7\%$. The strain dependence of L has been obtained from measuring $T_{1\rho}^{-1}$ as function of strain ε. The results are depicted in Fig. 8.

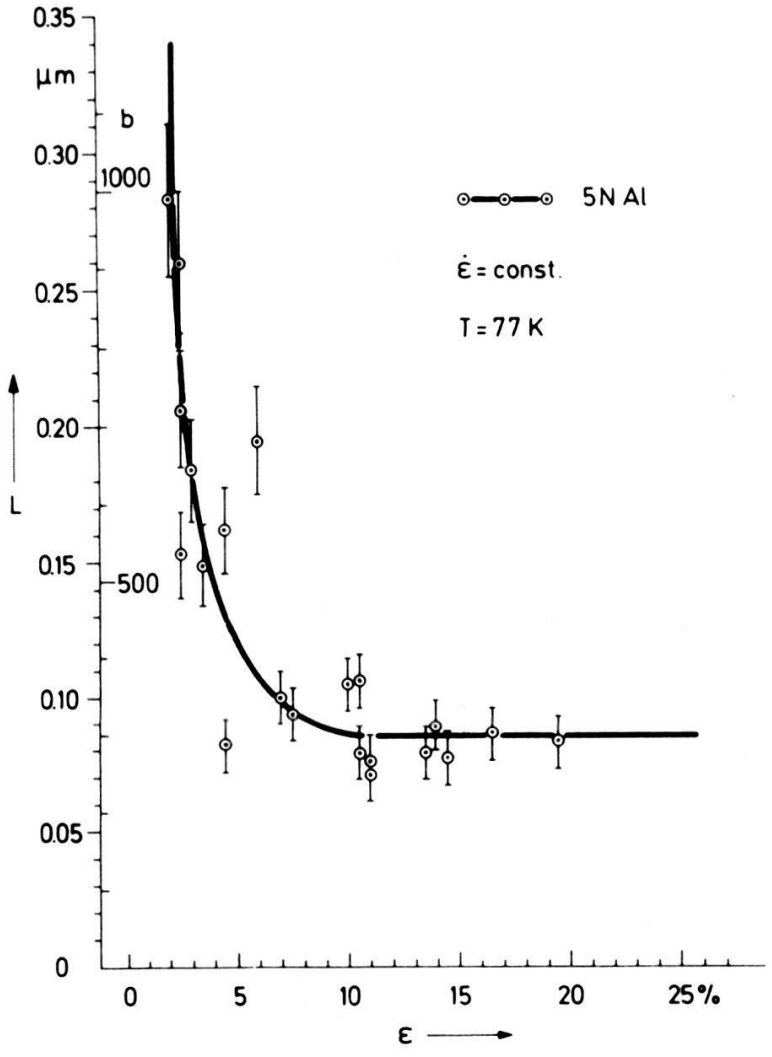

Fig. 8. The mean jump distance measured by NMR as a function of strain ε in Al.

The mean jump distance L measured by NMR in Al has to be interpreted with care in terms of mean slip distance and statistical slip length (Λ_{st}). As commonly found in annealed f.c.c. metals, a cell structure is formed in Al after deformation at room temperature and at 77K. Cell structure formation involves easy cross slip of large numbers of screw dislocations, i.e. either cross slip of screw dislocations from pile-ups behind Cottrell-Lomer barriers or cross slip from the original slip planed to form relatively strain free cell walls. Two electron micrographs illustrating the cell structure of deformed Al at 15% and at 25% strain are shown in Figs. 9 and 10, respectively. The cells are relatively free from dislocations but are separated by walls of high dislocation density. The dislocation aggregation in the cell walls are tangles, jogged, twisted and mixed together in an irregular way. The cell diameter is for both degrees of deformation ranging from 1 to 2 μm. The speed of the mobile dislocation is reduced in the cell wall compared with that outside the cell wall. As a result, the mean slip distance of dislocations is mainly determined by the cell size when the cell structure is well developed. The statistical slip length Λ_{st} will be of the same order of magnitude as the cell size ($\simeq$ 1-2 μm) i.e. much larger than the mean jump distance measured by NMR ($\simeq$ 0.1 μm for $\varepsilon \gtrsim 7\%$).

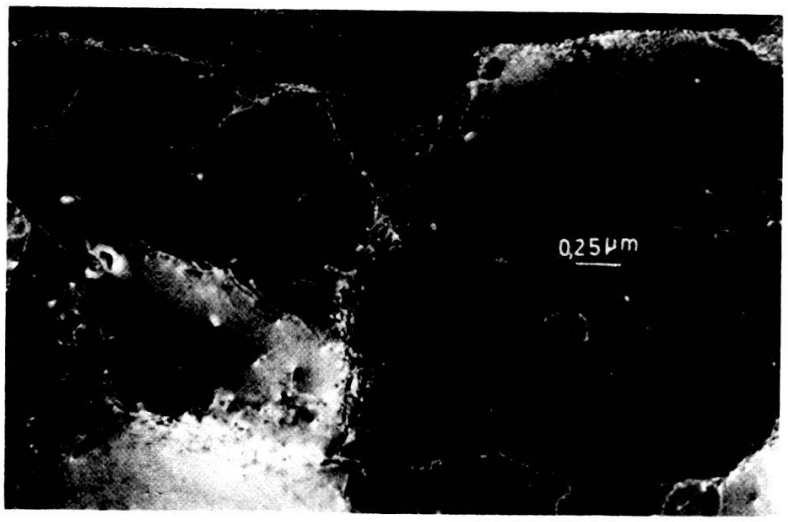

Fig. 9. Cell structure of Al deformed 15% at 77K. Dark field/weak beam image. [100] orientation, g=[002]; JEM 200 CX.

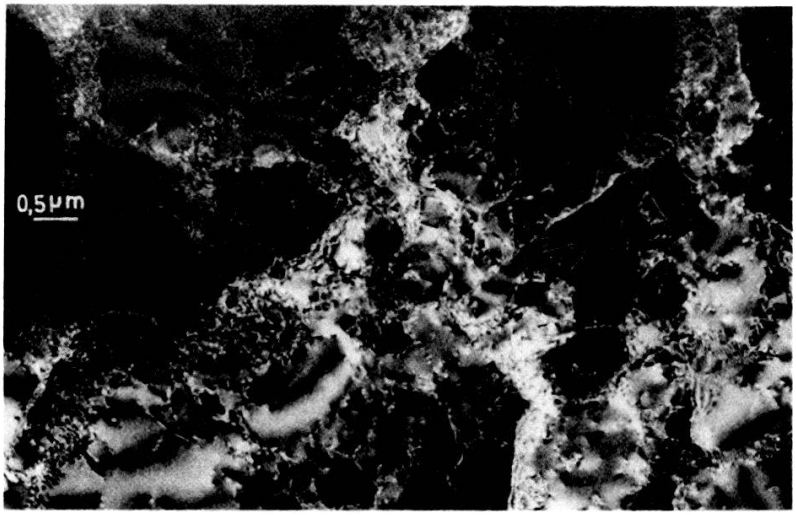

Fig. 10. Cell structure of Al deformed 25% at 77K. Dark field/weak beam image, [100] orientation, g=[002]; JEM 200 CX.

A plausible explanation for this difference is that all moving dislocations, present both in the cell boundary and in the interior region of the cell, affect the spin lattice relaxation rate. The mean jump distance of dislocations measured by NMR is possibly related to the spacing of the dislocation tangles near the cell boundary ranging from 0.01 to 0.1 µm. We assume the following model: a mobile dislocation crosses a cell by one step, i.e. the corresponding jump distance L_1 is of the order of the cell diameter ($\sim\Lambda_{st}$). Subsequently, many short jumps occur with a distance L_2 ($\simeq$ spacing of the tangles 0.01-0.1 µm). Assuming two different sets of corresponding mobile dislocation densities: ρ_1 in the interior of the cell and ρ_2 inside the cell wall the total spin lattice relaxation rate can be written as

$$\left(\frac{1}{T_{1\rho}}\right)_D = \left(\frac{1}{T_{1\rho}}\right)_D^{(1)} + \left(\frac{1}{T_{1\rho}}\right)_D^{(2)} \qquad (13)$$

where

$$\left(\frac{1}{T_{1\rho}}\right)_D^{(1)} \approx \frac{g_Q(L_1)\rho_1}{L_1\rho} \quad \text{and} \quad \left(\frac{1}{T_{1\rho}}\right)_D^{(2)} \approx \frac{g_Q(L_2)\rho_2}{L_2\rho} \qquad (14)$$

and $\rho = \rho_1 + \rho_2$. The dislocation density in the cell wall is about 5-6 times higher than in the interior region of the cell. Further, since $L_1 >> L_2$ and $g_Q(L_1) \simeq 1$ and $g_Q(L_2) \simeq 0.6$ (Fig. 1) the total spin lattice relaxation rate measured by NMR is largely determined by the jump distance inside the cell wall

$$\left(\frac{1}{T_{1\rho}}\right)_D \simeq \left(\frac{1}{T_{1\rho}}\right)_D^{(2)} \qquad (15)$$

Another explanation for the difference between the jump distance L measured by NMR and the mean slip distance Λ_{st} can be based on a dislocation mechanism in which the dislocation free path Λ_{st} depends on the mobile dislocation density and the number of dislocation intersections, N_c. If the dislocations are delayed at each of these intersections during a period of time $\tau_c > 10^{-4}$ s, spin-lattice relaxation takes place in the strong collision approximation, As a result the spin-lattice relaxation rate $T_{1\rho}^{-1}$ is determined by the waiting time τ_c at each intersection. The dislocation mean jump distance L thus obtained is much smaller than the actual mean slip distance Λ_{st}. When N_c is about 10 the mean jump distance L measured by NMR would be one order of magnitude smaller than Λ_{st} as observed. An argument that makes the former model somewhat favourable is that at small strains, i.e. before cells are being established, the mean jump distance is found to be much larger compared to L at large strains when distinct cells have been formed. In the former model one could expect that L decreases with increasing strains up to $\simeq$ 7% which is indeed the case (Fig. 8). At strains larger than 7%, the dislocation cells shrink in size through the subdivision of the largest cells. Such subdivision ceases the cells have become so small that no new cell walls are being nucleated because chance encounters of glide dislocations have become negligibly small. Therefore, the shrinking process of the cell pattern cannot go indefinitely and the cell diameter approaches an asymptotic value of 1-2 μm. It means that for strains larger than $\simeq$ 7% the statistical slip distance Λ_{st} and the mean jump distance L measured by NMR are almost not strain dependent.

5. Conclusion

It turned out that pulsed nuclear magnetic resonance is a complementary new technique for the study of moving dislocations in metallic and ionic crystals. Spin-lattice relaxation measurements indicate that moving dislocations cause fluctuations in the quadrupolar field. NMR experiments provide information of the microscopic mechanism of plastic deformation of solids.

Acknowledgement

The results presented here were obtained in collaboration with Prof. O. Kanert and his group of the University of Dortmund, FRG. This work is part of the research program of the Foundation for Fundamental Research on Matter (F.O.M.) and has been made possible by financial support from the Netherlands Organization for the Advancement of Pure Research (Z.W.O.- The Hague) and the Deutsche Forschungsgemeinschaft, Fed. Rep. Germany.

References

[1] J.Th.M. de Hosson, O. Kanert, A.W. Sleeswijk, in: Dislocations in Solids, Ed. F.R.N. Nabarro, North Holland Publ. Comp., 1983, vol. 6, Ch. 32, pp. 441-534.
[2] E. Orowan, Z. Phys. 89, 634 (1934).
[3] O. Kanert, M. Mehring, NMR, vol. 3, Springer Verlag, Berlin, 1971.
[4] O. Kanert, K. Preusser, Solid State Commun. 15, 97 (1974).
[5] J.Th.M. de Hosson, A. Huis in 't Veld, H. Tamler, O. Kanert, Acta Metall. 32, (1984).
[6] J.Th.M. de Hosson, O. Kanert, H. Tamler, Aluminium-Lithium alloys, AIME, 1983 (eds. T.H. Sanders and E.A. Starke).
[7] J.Th.M. de Hosson, W.H.M. Alsem, H. Tamler, O. Kanert, in: Defects, Fracture and Fatigue, Eds. G.C. Sih and J.W. Provan, Nijhoff, The Netherlands, 1982, p. 23.
[8] H. Tamler, O. Kanert, W.H.M. Alsem, J.Th.M. de Hosson, Acta Metall. 30, 1523 (1982).
[9] J.Th.M. de Hosson, O. Kanert, Materials Science Monograph, 20, Eds. V. Paidar and L. Lejcek, Elsevier, p. 75 (1984).
[10] W.H.M. Alsem, J.Th.M. de Hosson, Phil. Mag. 46, 327 (1982).
[11] W.H.M. Alsem, J.Th.M. de Hosson, R. Muenter, H. Tamler, O. Kanert, Phil. Mag. 46, 469 (1982).
[12] W.H.M. Alsem, J.Th.M. de Hosson, H. Tamler, O. Kanert, Phil. Mag. 46, 451 (1982).
[13] J.H. Van Vleck, Phys. Rev. 74, 1168 (1978).